Astron. Astrophys. 259, 453–461 (1992)

ASTRONOMY AND ASTROPHYSICS

Dynamos in discs and halos of galaxies

A. Brandenburg[1,2], K. J. Donner[2], D. Moss[3], A. Shukurov[4], D. D. Sokoloff[5], and I. Tuominen[2]

[1] NORDITA, Blegdamsvej 17, DK-2100 Copenhagen Ø, Denmark
[2] Observatory and Astrophysics Laboratory, University of Helsinki, Tähtitorninmäki, SF-00130 Helsinki, Finland
[3] Mathematics Department, The University, Manchester M13 9PL, UK
[4] IZMIRAN, Academy of Sciences, Troitsk 142092, Russia
[5] Department of Physics, Moscow University, Moscow 119899, Russia

Received September 18, 1991; accepted February 9, 1992

Abstract. We investigate linear and nonlinear dynamo models for a galactic disc embedded in a halo, assuming a relatively strong magnetic diffusivity and a non-vanishing α effect in the halo. We take the halo to be spherical and embedded in a vacuum. The field is assumed to be axisymmetric, but we do not impose symmetry conditions at the equatorial plane. In one parameter regime we find mixed parity solutions. However, it is argued that the regular magnetic field in the galactic halo can hardly reach a steady-state configuration during the galactic lifetime. In the regime that is observably relevant the field can have an even parity within and near the disc and an odd one in the halo. This may have implications for explaining the occurrence of a neutral sheet above the galactic plane. During certain time intervals the rotation measure of these models shows a doubly peaked azimuthal variation, which could be falsely interpreted as an indication of a bisymmetric field structure.

Key words: galaxies – magnetic fields – hydromagnetics – turbulence

1. Introduction

Recent observations provide evidence for the existence of magnetic fields of considerable strength in the halos of some galaxies (Sofue et al., 1986; Hummel et al., 1988; Beck, 1990, 1991a). Based on mixing length expressions for the α effect and the turbulent magnetic diffusivity, Ruzmaikin et al., (1988, Sect. VIII.1) and Sokoloff & Shukurov (1990) show that dynamo numbers are plausibly large enough to produce dynamo action in the halos of many galaxies. They argue further that a dynamo operating in a galaxy halo should produce odd parity, dipole-type, magnetic fields (A0). On the other hand, dynamos operating in the discs of galaxies should generate fields of even parity (i.e. quadrupole-type, S0). Sokoloff & Shukurov conjecture that for certain galaxies there might be an intermediate regime, where the overall field could have mixed parity.

The possibility of dynamo action in halos of galaxies may appear somewhat surprising. In the past twenty years, starting with the pioneering investigations of Parker (1971) and Vainshtein & Ruzmaikin (1971), galactic dynamo models have been elaborated where the dynamo solely operates in the discs of galaxies. Nevertheless, observations have indicated the possibility of strong turbulence in galaxy halos, the presence of which, together with rotation and a density gradient, is needed to cause an α effect to operate. In the present paper we accept this possibility and investigate the general features of such a model.

Up to now, ordered magnetic fields have been detected in the halos of three edge-on spiral galaxies, NGC 4631 (Hummel et al., 1988, 1991), NGC 891 (Hummel et al., 1991) and NGC 4565 (Sukumar and Allen, 1991). In these galaxies there is relatively highly polarised synchrotron emission present up to several kpc above the galactic disc. The regular magnetic field in the halo was interpreted as being associated with a galactic wind, that advects the field from the disc. This seemed reasonable in the case of NGC 4631, where the regular magnetic field is oriented predominantly in the radial direction. However, in the case of NGC 891 the field configuration is more complicated and the connection to a possible galactic wind is not so obvious. Meanwhile, Sokoloff & Shukurov (1990) suggest that the dominance of the radial component in the magnetic field structure can still be compatible with an $\alpha\Omega$ dynamo in the halo. Detailed comparison of the theory and observations of regular magnetic fields in galactic halos awaits determinations of Faraday rotation measures produced in the halos. In this paper we analyse a dynamo model which includes basic elements of the complex physical system formed by the disc and the gaseous halo, with both components as sites of dynamo activity. Within the present approach, such processes as galactic fountains, chimneys, turbulence, etc. are parameterised using the concepts of turbulent magnetic diffusivity and mean helicity.

Our analysis here is motivated by the following questions. An approximate solution for the spherical dynamo by Sokoloff & Shukurov (1990) has shown that dynamo action in galactic halos is feasible, but it remains necessary to obtain more accurate, numerical estimates of the generation threshold, with allowance for more complicated spatial distributions of the turbulent magnetic diffusivity, mean helicity, etc.

Secondly, qualitative analysis of the dynamo was based on the presumption that the galactic disc and the halo host independent dynamos. This approach is valid only as a first approximation. In reality, the disc and the halo constitute a single dynamo system. The disc preferably generates an even field while in the halo odd parity fields dominate (e.g. Stix, 1975). Then the following

Send offprint requests to: A. Brandenburg, NORDITA

problem arises. Acting separately, the dynamos in the disc and the halo would generate large-scale fields of different parities (even and odd, respectively) and different temporal behaviours (steady and oscillatory, respectively). The resulting overall field might be expected to have a mixed parity provided the magnetic connection between the disc and the halo is weak. On the other hand, the α-effect, differential rotation and turbulent diffusivity show certain symmetries about the equator, which are the same for both the disc and the halo, and there are therefore only pure parity eigensolutions for the kinematic dynamo problem.

Our results for a more realistic galactic dynamo model, presented in Sects. 6 and 7, resolve this problem as follows. The turbulent magnetic diffusion time in the halo exceeds the Hubble time. Therefore, we expect that the odd parity of the overall field, imposed by the halo, cannot be fully established during the galactic lifetime and that the fields observed in the galactic halos represent an intermediate stage of evolution: at early stages a rapidly growing even field generated in the disc dominates in the disc neighbourhood while asymptotically the overall field has an odd parity. Numerical solutions of this type are discussed in Sect. 7.2 below. This makes it clear that models of the disc dynamo in which the halo does not play an active role are quite adequate in many respects. The ultimate field parity is, usually, either of purely odd or even parity, depending on whether the halo or the disc generates field more efficiently. We should stress, however, that there are also stable mixed-parity nonlinear solutions which are realised for a rather narrow range of the values of the relevant parameters.

We assume the halo to be spherical and embedded in a vacuum (cf. Elstner et al., 1990). We impose vacuum boundary conditions at the surface of the halo as in the theory of solar and stellar dynamos. In an initial experiment we model the dynamo in the disc by imposing an ad hoc "ring current" in a central region which has an associated field with S0-parity, and study how this will influence the parity of the global preferred mode. Subsequently we investigate both linear and nonlinear dynamo models with "flat" distributions for the turbulent magnetic diffusivity. In some cases we also include the effects of the disc on the α effect. The field generated by the flat disc alone is typically of S0 parity. However, in the presence of the halo the field in the disc is coupled to that in the halo and we have therefore to solve the dynamo equations for the whole system. Only a subsequent stability analysis can reveal whether the parity of the ultimate field belonging to a stable solution is S0, A0, or a mixture of both. We restrict ourselves to purely axisymmetric solutions. Experience from previous investigations (e.g. Jennings et al., 1990) suggests that, at least with an axisymmetric α effect, nonaxisymmetric modes are unstable if a certain, plausible, amount of differential rotation is present. We thus do not address the problem of generation of nonaxisymmetric ($m = 1$) galactic fields.

2. Turbulence parameters for disc and halo

Before we consider detailed models let us first discuss the parameters relevant to an estimation of the strength of dynamo action in both the disc and the halo of typical galaxies. As an order of magnitude estimate we assume for the turbulent magnetic diffusivity $\eta = \frac{1}{3}u_t\ell$, where u_t is the rms velocity of the turbulence and ℓ the correlation length. The α effect is assumed to be proportional to $\hat{\alpha} = \Omega_0\ell$, where Ω_0 is the angular velocity at some characteristic radius. The expression routinely used in the galactic dynamo theory, which differs from this by an additional factor ℓ/h, where h is the scale height of the disc (Ruzmaikin et al., 1988), can be justified only for thin discs. We give some values for various relevant quantities in Table 1. As an example we assume a linear velocity of 150 km/s at a radius of 5 kpc, so we take $\Omega_0 = 10^{-15}\,\mathrm{s}^{-1}$ when calculating α. The dimensionless strength of the α-effect is measured by the usual dynamo parameter

$$C_\alpha = \alpha_0 R/\eta_{\mathrm{halo}}, \tag{1}$$

where η_{halo} is the value of η in the halo, R is the halo radius, and α_0 a typical value of α (see below). We also give the value of the quantity

$$C_\Omega = \Omega_0 R^2/\eta_{\mathrm{halo}}, \tag{2}$$

which measures the strength of the Ω-effect.

Table 1. Parameters characterising the turbulence in the disc and in the halo of typical galaxies with $\Omega = 10^{-15}\,\mathrm{s}^{-1}$ and $R = 15$ kpc

quantity	disc	halo
ℓ	100 pc	500 pc
u_t	10 km/s	100 km/s
η	$10^{26}\,\mathrm{cm}^2/\mathrm{s}$	$5\,10^{27}\,\mathrm{cm}^2/\mathrm{s}$
$\hat{\alpha}$	$3\,10^5$ cm/s	10^6 cm/s
$\hat{\alpha}R/\eta_{\mathrm{halo}}$	3	9
C_Ω	400	

The critical values of C_α for a sphere with uniform η and α proportional to $\cos\theta$ (see below) are less than ten even for $C_\Omega = 0$, so the values given in Table 1 are likely to be supercritical. The numbers given in this table even suggest that α in the halo is larger than in the disc. Note that the opposite was actually assumed in earlier investigations of thick-disc galaxies (e.g. Moss & Tuominen, 1990; Donner & Brandenburg, 1990). There is, however, a large uncertainty concerning the appropriate values of the relevant parameters. For this reason we shall also consider models with slightly different parameters to those in Table 1.

3. An embedded disc model

In order to specify a model we have to prescribe the magnetic diffusivity η, the coefficient α, and the rotational angular velocity Ω as functions of the cylindrical polar coordinates ϖ, z. We also use spherical polar coordinates r, θ, which are related to the cylindrical by $\varpi = r\sin\theta$ and $z = r\cos\theta$.

The angular velocity Ω is assumed to depend only on ϖ with

$$\Omega(\varpi) = \Omega_0\left[1 + \left(\frac{\varpi}{\varpi_0}\right)^2\right]^{-1/2}. \tag{3}$$

We take $\varpi_0 = 0.3$, which corresponds to about 5 kpc, if $R = 15$ kpc; see Sokoloff & Shukurov (1990) for discussion of the appropriate value of R.

In order to include the effect of the disc we make η and α depend on the height z above the galactic plane. We take

$$\eta(z) = \eta_0 - \eta_1\, e^{-(z/z_\eta)^2}. \tag{4}$$

The diffusivities in the disc and high in the halo are respectively $\eta_{\rm disc} = \eta_0 - \eta_1$ and $\eta_{\rm halo} = \eta_0$ since $z_\eta \ll R$. In most of the cases considered below we assume $\eta_1 > 0$, i.e. $\eta_{\rm disc} < \eta_{\rm halo}$. We take $z_\eta = 0.2$ in all cases, or 3 kpc in dimensional units. This value certainly exceeds the real disc half-thickness, but this represents approximately a lower limit for an accurate solution with the grid resolution adopted (see below).

We assume also a non-spherical α-profile, given by

$$\alpha(\varpi, z, t) = \frac{\tilde{\alpha}}{1 + \alpha_B \boldsymbol{B}^2(\varpi, z, t)} \left[\alpha_0 + \alpha_1 - 2\alpha_1 e^{-(z/z_\alpha)^2}\right]. \quad (5)$$

Here, α_B denotes the strength of the α-quenching feedback. In most of the cases we take $\tilde{\alpha} = \cos\theta$, giving a discontinuity at $\varpi = z = 0$, that does not, however, lead to a singularity in the dynamo equations (Roberts, 1972). In some cases we take $\tilde{\alpha} = z$ instead. High in the halo the value of $\hat{\alpha}$ (the term in square brackets in Eq. (5)) is $\alpha_0 + \alpha_1$, and in the disc it is $\alpha_0 - \alpha_1$. The values of Table 1 can be reproduced with $C_\alpha = 6$ and $\alpha_1/\alpha_0 = 0.5$.

4. The dynamo equations

The dynamo equation governing the evolution of the average (ordered) magnetic field $\boldsymbol{B}$ is

$$\frac{\partial \boldsymbol{B}}{\partial t} = \mathrm{curl}\,(\boldsymbol{u} \times \boldsymbol{B} + \alpha \boldsymbol{B} - \boldsymbol{J}/\sigma), \quad \mathrm{div}\,\boldsymbol{B} = 0. \quad (6)$$

Here, $\boldsymbol{J} = \mathrm{curl}\,\boldsymbol{B}/\mu_0$ is the electrical current, μ_0 the induction constant, and σ the electric (turbulent) conductivity. The magnetic diffusivity is given by $\eta = 1/\sigma\mu_0$.

We introduce non-dimensional variables by measuring ϖ and z in units of the radius of the galactic halo R, and time t in magnetic diffusion times $R^2/\eta_{\rm halo}$. The units for the other non-dimensional variables are

$$[\boldsymbol{u}] = \eta_{\rm halo}/R, \quad [\boldsymbol{B}] = [\boldsymbol{u}](\mu_0\bar{\rho})^{1/2}, \quad [\boldsymbol{J}] = [\boldsymbol{B}]/\mu_0 R. \quad (7)$$

Using the quantities of Table 1 we have $[t] \approx 1.3\,10^{10}$ yr, $[\boldsymbol{u}] \approx 1$ km/s, and with $\rho \approx 2\,10^{-24}$ g/cm^3 the unit of magnetic field is $[\boldsymbol{B}] \approx 0.5\alpha_B^{-1/2}\,\mu$G. Since α quenching is the only nonlinearity in our model, if α_B is constant we can take $\alpha_B = 1$, without loss of generality.

We assume the magnetic field to be symmetric about the rotation axis and so we can represent the field as $\boldsymbol{B} = b\hat{\boldsymbol{\phi}} + \mathrm{curl}\,(a\hat{\boldsymbol{\phi}})$ and the electric current as $\boldsymbol{J} = j\hat{\boldsymbol{\phi}} + \mathrm{curl}\,(b\hat{\boldsymbol{\phi}})$, where $j = -D^2 a$ and $D^2 a = -\hat{\boldsymbol{\phi}} \cdot \mathrm{curl}\,\mathrm{curl}\,(a\hat{\boldsymbol{\phi}})$. In this paper we neglect poloidal flows and take $\boldsymbol{u} = \hat{\boldsymbol{\phi}}\varpi\Omega$. The dynamo equations for a and b are then

$$(\partial_t - \eta D^2)a = \alpha b, \quad (8)$$

$$(\partial_t - \eta D^2)b = \alpha j + \hat{\boldsymbol{\phi}} \cdot [\nabla\alpha \times \boldsymbol{B}_p - \nabla\eta \times \boldsymbol{J}_p] + \varpi \boldsymbol{B}_p \cdot \nabla\Omega. \quad (9)$$

We solve Eqs. (8) and (9) in spherical geometry on a finite difference grid in the r, θ plane in the range $0 \le r \le 1$ and $0 \le \theta \le \pi$. Here, r is the distance from the center and θ is the polar angle (colatitude). The boundary condition imposed on $r = R$ is that $\boldsymbol{B}$ fits on to a potential field in $r > R$. The grid resolution adopted is 21×41 points, with a normal timestep of 2×10^{-4}. Further details of the method are given in Brandenburg et al. (1989).

The linear results reported in Sect. 6 are computed by an expansion into spherical harmonics, using finite differences in the radial direction. For these calculations the Gaussians in Eqs. (4) and (5) are replaced by a parabola, i.e.

$$e^{-z^2} \to \begin{cases} 1 - z^2, & |z| < 1, \\ 0, & \text{otherwise.} \end{cases} \quad (10)$$

We then expand the resulting η and α profiles in Legendre polynomials to fourth and fifth order, respectively. Furthermore, in the linear calculations we use a slightly modified rotation law in the halo. We write the angular velocity as a fourth order polynomial in $\cos\theta$, and choose the radial dependence of the coefficients to give an Ω that is nearly independent of z near the plane of the disc. The surfaces of constant angular velocity of the resulting rotation law are closed prolate surfaces that are almost cylindrical up to a latitude of about 50° above the disc plane. The two codes give consistently similar results for the linear case ($\alpha_B \equiv 0$), although the actual numbers for the growth rates can differ somewhat; see Sect. 6. We need to use this strictly linear code in order to compute growth rates of modes other than the most rapidly growing.

Note that we do *not* neglect the α effect for the generation of toroidal field from a poloidal one in Eq. (9), i.e. we consider an $\alpha^2\Omega$ dynamo, as opposed to the often adopted $\alpha\Omega$ dynamo approximation.

5. A ring current experiment

We have above discussed the possibility that a spherical dynamo, in which a A0 mode is naturally excited, may be forced into a mixed parity configuration by the presence of an embedded disc dynamo that itself has a preference for a S0 mode. In order to investigate in a simple way the plausibility and consequences of such a mechanism a simple numerical experiment was devised.

In this section we consider a spherical dynamo system with homogeneous diffusivity, no differential rotation and $\alpha = \alpha_0 \cos\theta$. The first growing mode in such a system is of A0 type and is excited when the dynamo parameter $C_\alpha = 7.64$. The first S0 mode is excited at $C_\alpha = 7.81$. Now, in addition, we introduce an ad hoc, inexorable "ring current", $\boldsymbol{j}_R = j_R\hat{\boldsymbol{\phi}}$, with

$$j_R = j_0 r^4 (r_0 - r)\sin\theta\cos\theta, \quad r < r_0, \qquad j_R = 0, \quad r > r_0, \quad (11)$$

which gives an additional term j_R on the right hand side of Eq. (8). We take $r_0 = 0.3$, so that this current is confined to the central regions. An even parity (quadrupolar) poloidal field is generated, which we consider as simulating the effects of an inner dynamo generating a S0 type field, embedded in a spherical dynamo in which the preferred mode is of A0 type.

Because of the presence of a ring current the system of equations (8) and (9) becomes inhomogeneous, and so we cannot strictly speak of a dynamo, as an external electromotive force drives the current $\boldsymbol{j}_R$. If $C_\alpha = 0$, then for any value of j_0 we can find a diffusion-limited equilibrium state of even parity, with field strength proportional to j_0. This field will be concentrated to the inner part of the spherical volume, as is j_R, and will be of very different structure to the global dynamo modes. This field by itself is of little interest but it allows us to investigate, at a qualitative level, the plausible effect of the even-parity magnetic field in the inner (smaller) part of the dynamo volume on the odd parity global field that is excited at $C_\alpha = 7.64$ when $j_0 = 0$ (we recognise that even for $C_\alpha = 0$ an even parity field will be present, associated with the current $\boldsymbol{j}_R$.) We emphasize that the introduction of this "ring current" is solely a computational device to mimic the presence of an independent "inner" dynamo of opposite parity to the most readily excited global mode.

In Table 2 we give critical values of C_α for solutions that bifurcate from the ring current solution for various values of j_0. We also give the corresponding values of the parity parameter defined as

$$P = [E^{(S)} - E^{(A)}]/[E^{(S)} + E^{(A)}], \quad (12)$$

Here, $E = \int \boldsymbol{B}^2/2\mu_0\, dV$ is the magnetic energy and the labels S and A refer to the energies of the symmetric and antisymmetric parts of the field. Note that the critical value $C_\alpha = 7.64$ referred to above is calculated as 7.62 at the accuracy of our computations (usually 21×41 mesh points in the r and θ directions, respectively).

Table 2. Marginal dynamo numbers $C_\alpha^{\rm crit}$ and parity parameter P in the final state for various values of j_0

j_0	$C_\alpha^{\rm crit}$	P
0.0	7.62	−1.000
$3\,10^3$	7.62	−1.000
$1\,10^4$	7.62	−0.985
$2\,10^4$	7.62	−0.928
$5\,10^4$	7.62	−0.629
$1\,10^5$	7.62	+0.468
$2\,10^5$	6.99	+1.000
$1\,10^6$	5.57	+1.000

For small values of j_0 the dynamo field that is excited has P very close to −1 while the critical value of C_α is indistinguishable from that without the ring current. For sufficiently large j_0, $P = +1$. For intermediate values, $j_0 = 10^{4...5}$, $P \to -0.99.... + 0.5$. We deduce that for significantly smaller nonzero values of j_0, P is close to, but not exactly equal to, −1 (since there is inevitably an even parity field component proportional to j_0). It appears that for a strong enough quadrupolar ring current (i.e. a strong enough "inner" dynamo) the most easily excited mode of the "outer" dynamo can switch from A0 to S0 type. For values of j_0 of $O(10^4)$ a mixed parity field is clearly present, with the S0 component from the imposed current imposing its structure on the "outer" dynamo which is intrinsically of A0 type.

Of course, this model does not reproduce all the features of a disc dynamo embedded in a spherical halo and, in particular, we have prescribed a quadrupolar inner field irrespective of the outer conditions. We might anticipate that for a large enough ratio of outer to inner dynamo strengths a self consistently computed inner dynamo might switch *its* preferred mode to A0. This possibility is not available in our restricted model. Thus, the experiment does suggest, but not rigorously establish, the possibility of mixed modes being excited for intermediate values of the relative strength of the dynamo in the disc. Furthermore it is plausible that an embedded (disc) dynamo can change the parity of the field of the embedding halo, in this case from $P = -1$ to $P = +1$.

For the remainder of the paper we only consider "true" dynamo solutions without ring current.

6. Results in the linear regime

Linear theory is valid as long as the magnetic field strength is sufficiently weak. Thus, linear growth rates are useful to estimate the relative importance of oscillatory and non-oscillatory modes with different symmetry properties before nonlinear saturation sets in. For galaxies this may only happen after a substantial fraction of the Hubble time (see below). Once saturation sets in, it is only in the very weakly nonlinear regime that determination of the mode with the smallest critical dynamo number is relevant for establishing the symmetry of the stable field (Krause & Meinel 1988). For larger C_α the nonlinear equations have to be solved (see Sect. 7). Here we take $\alpha_1 = 0$, i.e. no effects of the disc on the α effect.

The dependence of the growth rate on the prominence of the disc, i.e. on the value of η_1, is shown in Table 3. As expected, when the dynamo in the disc dominates, the fastest growing modes are non-oscillatory. (For large enough values of C_α dipole and quadrupole modes become asymptotically equally excited, see Table 4 and Brandenburg et al., 1989.) For our α profile these modes are confined to the centre of the galaxy. With a less centrally peaked profile they would extend to larger radii, but would also be more difficult to excite. The existence and importance of this type of mode were discussed in Donner & Brandenburg (1990).

Table 3. Growth rates as functions of η_1 with $C_\alpha = 9$, for $C_\Omega = 400$ and 600, $\alpha_1 = 0$, $\tilde{\alpha} = \cos\theta$. The most rapidly growing modes are indicated in boldface. The last column gives the growth rate of the fastest growing mode obtained from the mesh point code using a 41×41 grid. (The differences between the two codes arise mainly from the approximation in representing Ω when using spherical harmonics, see Sect. 4)

C_Ω	η_1	S0	$S0_{osc}$	A0	$A0_{osc}$	mesh point
400	0.95	64.1	2.7	**67.7**	4.4	73. $A0_{st}$
400	0.8	−5.0	**2.0**	−57.0	1.9	5.3 $A0_{osc}$
600	0.95	64.9	4.2	**67.7**	8.4	73. $A0_{st}$
600	0.9	**11.3**	3.4	−6.1	7.2	15. $S0_{st}$
600	0.8	−1.9	2.3	−44.0	**5.6**	9.0 $A0_{osc}$
600	0.6	−7.9	1.2	−52.3	**3.6**	6.7 $A0_{osc}$
600	0.4	−10.8	0.4	−60.0	**2.4**	5.2 $A0_{osc}$
600	0.2	−13.2	−0.2	−67.7	**1.4**	4.0 $A0_{osc}$
600	0.0	−15.9	−0.5	−84.8	**0.8**	3.0 $A0_{osc}$

The oscillatory modes have a completely different spatial structure with large field strength high in the halo. As we will see later, after the growth of the central modes is halted by nonlinear effects the oscillating dipole solution begins to dominate in a larger volume encompassing the halo and the major portion of the disc. For weaker discs, the oscillating dipole modes have the largest growth rates.

Table 4 gives the growth rates as functions of the strength of the α-effect. Note the strong dependence of the non-oscillatory A0 modes on C_α, which is consistent with their generation by the α^2 mechanism. The disc S0 modes are less sensitive in this respect.

Finally we give the critical values of C_α for selected parameter values in Table 5. It is seen that the steady S0 modes are most easily excited when the disc is prominent. Otherwise the oscillatory halo modes are preferred.

In Tables 3 and 5 we have included some results obtained with the mesh point code for comparison. The results from the two methods are in qualitative and rough quantitative agreement. The quantitative differences can be understood on the basis of the differences of the models adopted in the two cases. In particular, because the same nominal disc thickness z_η was assumed in both

Table 4. Growth rates as functions of C_α with $\eta_1 = 0.95$, for $C_\Omega = 400$ and 600, $\alpha_1 = 0$, $\tilde{\alpha} = \cos\theta$. The most rapidly growing modes are indicated in boldface

C_Ω	C_α	S0	$S0_{osc}$	A0	$A0_{osc}$
400	5	**0.7**	−48.8	−19.3	−4.4
400	7	**11.4**	−4.5	10.6	−0.4
400	9	64.1	2.7	**67.7**	4.4
600	4	**0.1**	−20.0	−29.1	−4.3
600	5	**2.2**	−14.8	−24.2	−2.0
600	6	**5.5**	−9.0	−9.8	0.4
600	7	**14.1**	−4.2	9.3	3.0
600	8	33.2	0.7	**35.2**	5.7
600	9	64.9	4.2	**67.7**	8.4
600	10	107.3	8.2	**110.3**	11.4
600	11	159.5	12.3	**162.4**	14.5
600	12	221.4	16.3	**224.0**	17.7

Table 5. Critical values of C_α for $C_\Omega = 400$ and 600, $\eta_1 = 0.95$ and 0.8, $\alpha_1 = 0$, $\tilde{\alpha} = \cos\theta$. The most easily excited modes are indicated in boldface. Numbers in parentheses indicate that the first growing non-oscillatory mode is produced by the merging of two growing oscillatory modes. The last column gives the critical values obtained from the mesh point code using a 41 × 41 grid

C_Ω	η_1	S0	$S0_{osc}$	A0	$A0_{osc}$	mesh point
400	0.95	**4.5**	8.3	6.5	7.2	ca. 2.5 $S0_{st}$
400	0.8	10.4	8.5	(12)	**8.3**	ca. 7.5 $A0_{osc}$
600	0.95	**4.0**	7.8	6.5	5.8	ca. 2.0 $S0_{st}$
600	0.8	9.6	8.4	(13.5)	**7.1**	ca. 6.4 $A0_{osc}$

calculations, the disc was effectively thinner in the linear case; see Sect. 4. For example, choosing the value $z_\eta = 0.27$ instead of 0.20 would give the same value of $\int \eta dz$ in both models. Using this value of z_η the critical values of C_α obtained from the linear code change to respectively 2.1 and 1.5 for $C_\Omega = 400$ and 600, and $\eta_1 = 0.95$.

7. Results in the nonlinear regime

We now present finite amplitude results where the field strength is limited by nonlinear effects. In all the cases considered below we choose $\eta_1 = 0.95$, which is approximately the largest possible value attainable with our standard resolution of 21 × 41 mesh points. In some cases we checked our results using a resolution of 41 × 81 mesh points and typically found that the solution was not significantly changed. The stability behaviour of these solutions is investigated by adding a small perturbation of opposite parity. As initial condition we assume either a random field or we take for a a superposition of terms proportional to $P_1^1(\cos\theta)$ and $P_2^1(\cos\theta)$; see Sect. 7.2.

7.1. Amplitude and stability of solutions

First we discuss the results for $\tilde{\alpha} = \cos\theta$ and $\alpha_1 = 0$. For both $C_\Omega = 400$ and 600 a steady S0 solution is most easily excited. In the interval $2 \lesssim C_\alpha \lesssim 6$ the S0 solution is stable, but the energy is small and does not significantly change with C_α. The magnetic field is concentrated into the disc. At $C_\alpha \gtrsim 6$ a stable A0 solution is found, with a relatively strong magnetic field that extends into the halo. For $C_\Omega = 400$ this A0 solution is stable for all larger values of C_α considered ($C_\alpha \leq 15$), whilst the S0 solution is unstable. For $C_\Omega = 600$, the A0 solution is only stable in the interval $6 \lesssim C_\alpha \lesssim 10$ and becomes unstable for $C_\alpha \approx 10$. For larger values of C_α we find only a stable S0 solution. However, for intermediate values of C_α there is a stable mixed parity solution (denoted by M) for this C_Ω. This solution connects with the S0 solution. Apparently the mixed parity solution does not directly bifurcate from the A0 solution but rather evolves via some other unstable solution. Such solutions usually cannot be computed by timestepping methods (cf. Jennings, 1991). The evolution of the parity parameter for the quasiperiodic mixed parity solution is shown in Fig. 2. The unstable S0 solution is steady for small values of C_α, but it becomes oscillatory for even slightly supercritical values. The A0 solution is always oscillatory. The bifurcation diagrams for $C_\Omega = 400$ and 600 are shown in the upper and lower panels of Fig. 1. With the parameters given in Table 1 $C_\Omega = 600$ corresponds to a linear velocity of about 200 km/s.

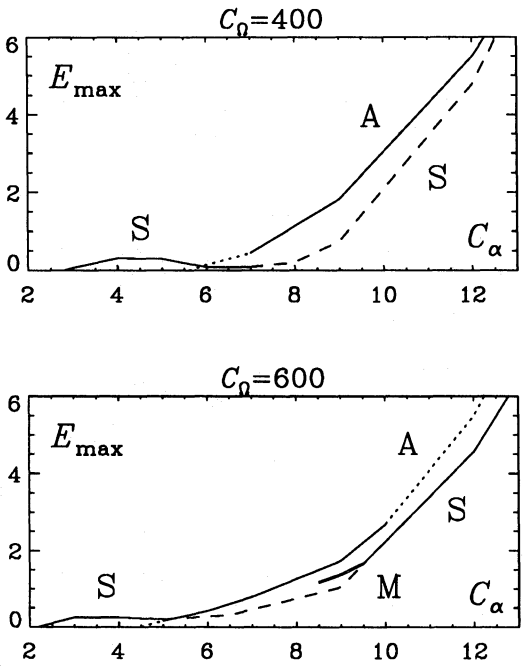

Fig. 1. Bifurcation diagram for $C_\Omega = 400$ (upper panel) and 600 (lower panel). Stable solutions are denoted by solid lines and unstable ones by dotted and dashed lines lines. $\eta_1 = 0.95$, $\alpha_1 = 0$, $\tilde{\alpha} = \cos\theta$

For $\tilde{\alpha} = z$ the numbers change slightly, but the overall bifurcation structure is not much affected. Also the mixed parity solution still exists (see Table 6).

We expect that the S0 solution will become stable (at least for small values of C_α) when the α effect is more concentrated to the disc, i.e. as $\alpha_1 \to -\alpha_0$. In order to confirm this we computed solutions for different values of α_1, and these are summarised in Table 6. For both $C_\Omega = 400$ and 600 there is a stable steady S0 solution for negative values of α_1 and an oscillatory A0 solution for $\alpha_1 \geq 0$.

7.2. The initial growth phase

The typical time scales for galaxies are so long that any dynamo in the galactic halo has not necessarily had enough time to evolve

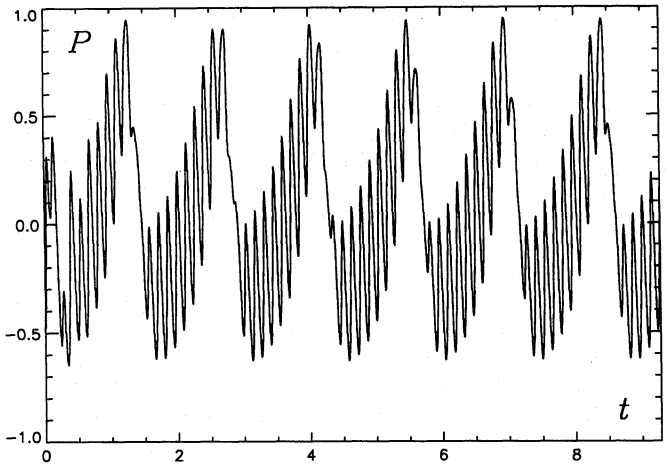

Fig. 2. Evolution of the parity parameter P for the quasiperiodic mixed parity solution. $C_\alpha = 9$, $C_\Omega = 600$, $\eta_1 = 0.95$, $\alpha_1 = 0$, $\tilde{\alpha} = \cos\theta$

Table 6. Maximum energy and period (in brackets) of solutions for different values of α_1, C_Ω, and C_α for $\eta_1 = 0.95$ and for the two cases $\tilde{\alpha} = \cos\theta$ and $\tilde{\alpha} = z$. Stable solutions are shown in boldface

			$\tilde{\alpha} = \cos\theta$		
α_1	C_Ω	C_α	A0	S0	Mixed
−1	400	12	0.18 (0.29)	**5.02**(∞)	
0	400	12	**5.61 (0.61)**	4.75 (0.48)	
1	400	12	**22.0 (1.12)**	30.2 (0.78)	
−1	600	9	0.16 (0.24)	**5.92**(∞)	
0	600	9	**1.78 (0.29)**	1.04 (0.26)	**1.42 (0.28)**
1	600	9	**13.3 (0.42)**	12.4 (0.37)	
			$\tilde{\alpha} = z$		
−1	400	12	0	**1.72**(∞)	
0	400	12	**1.74 (0.54)**	0.45 (0.44)	
1	400	12	**15.3 (1.23)**	25.0 (1.07)	
−1	600	12	0	**3.61**(∞)	
0	600	12	**1.68 (0.33)**	0.96 (0.27)	**1.16 (0.27)**
1	600	12	**20.7 (0.62)**	20.6 (0.48)	

to a stable configuration and therefore memories of the initial field configuration may still persist after several Hubble times.

In our most studied model the turbulent conductivity in the disc is much larger than in the halo. We expect therefore that the field will grow more rapidly in the disc until nonlinear saturation inhibits further field growth. The field produced in the disc typically is of S0 parity. When C_α is not too large and α_1 is non-negative the S0 field is unstable and eventually the A0 field will dominate (see Fig. 1). In order to quantify this process we define the (dimensionless) magnetic field energy separately for disc and halo as

$$E_{\rm disc} = \frac{1}{2}\int e^{-(z/z_B)^2}\,\boldsymbol{B}^2\,dV, \quad E_{\rm halo} = E - E_{\rm disc}. \tag{13}$$

This definition of $E_{\rm disc}$ was chosen for computational convenience, but is not critical. By measuring separately the energies contained in the symmetric and antisymmetric part of the field we can define parity parameters for disc and halo, $P_{\rm disc}$ and $P_{\rm halo}$ similarly to Eq. (12). We choose $z_B = 0.2$ $(= z_\alpha = z_\eta)$.

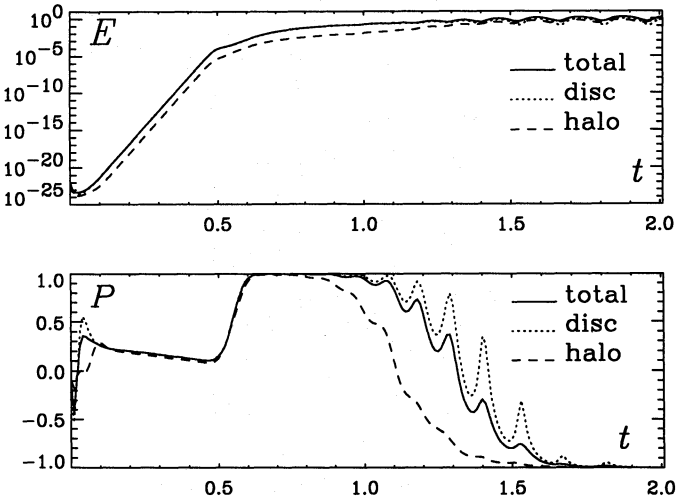

Fig. 3. Evolution of E, $E_{\rm disc}$, $E_{\rm halo}$ (upper panel) and P, $P_{\rm disc}$, $P_{\rm halo}$ for a weak initial seed magnetic field. $C_\alpha = 9$, $C_\Omega = 600$, $\eta_1 = 0.95$, $\alpha_1 = 0$, $\tilde{\alpha} = \cos\theta$

In Fig. 3 we show the evolution of E, $E_{\rm disc}$, $E_{\rm halo}$, P, $P_{\rm disc}$, $P_{\rm halo}$ for a weak initial seed magnetic field for one particular choice of parameters. During the interval $t = 0.05 - 0.5$ the field energy grows with a maximal rate of 40 decades per time unit (≈ 1 Hubble time), which is consistent with the linear growth rates of the fastest growing modes obtained in Sect. 6. Because the growth rate of the A0 mode is slightly larger, the parity decreases slowly. However, the critical value of C_α is smaller for the S0 mode (see Table 5), which can therefore continue to grow after growth of the A0 mode has saturated. The parity then rapidly changes to +1. Figure 3 thus confirms the idea that the field is generated at first in the disc. After approximately one time unit the field in the halo becomes significant and the overall field becomes oscillatory and flips to A0 parity. The process of parity flip occurs somewhat earlier if the initial field is stronger.

7.3. Sensitivity to initial conditions

We have considered the initial phase for the case with $C_\Omega = 600$ and $C_\alpha = 9$. It turns out that the magnetic field evolution can depend quite sensitively on the form of the initial seed field. Normally we assume a superposition of two pure parity states with

$$a(r,\theta) = a_0 r[(1-p)P_1^1(\cos\theta) + (1+p)P_2^1(\cos\theta)], \tag{14}$$

where a_0 is a scaling factor. Note that the initial parity parameter $P(0)$ coincides with p only in the pure parity cases $p = \pm 1$, but not for intermediate values. We also made some runs with a random initial field (cf. Ruzmaikin et al., 1988, Sect. VII.14), given by

$$a(\varpi,z) = \sum_{i=1}^{100} a_0\epsilon_i \exp[-(\varpi-\varpi_i)^2/d_0^2 - (z-z_i)^2/d_0^2], \tag{15}$$

where ϵ_i, ϖ_i, and z_i are random numbers between zero and unity. d_0 is the typical spatial scale of the initial perturbation, for which we always took the value $d_0 = 0.05$ (corresponding to 750 pc). The evolution of the parity parameter P for different initial conditions is shown in Fig. 4. The solid lines are for initial conditions using Eq. (14) with $p = -0.9$, -0.5, and 0 whilst broken lines are for

Eq. (15) with different sets of random numbers. The intermediate phase of the S0 field dominance is strongly suppressed, when the initial field parity is close to $P = -1$.

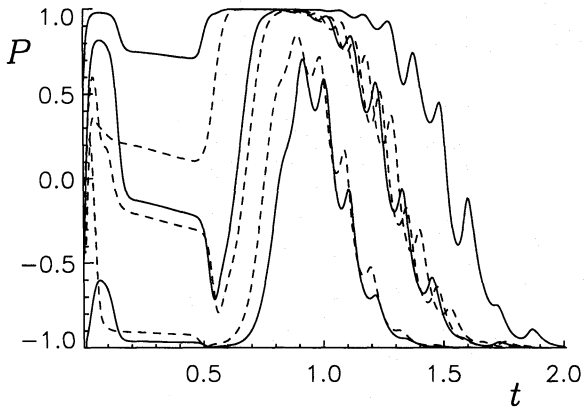

Fig. 4. Evolution of the parity parameter P for different initial conditions. $C_\alpha = 9$, $C_\Omega = 600$, $\eta_1 = 0.95$ $\alpha_1 = 0$, $\tilde{\alpha} = \cos\theta$

7.4. Field geometry and rotation measure

The magnetic fields of galaxies can only be observed via polarisation measurements. It is therefore interesting to present observable distributions associated with our solutions. We have computed the variation with time of the rotation measure RM for the nonlinear mixed parity solution with $C_\alpha = 9$, $C_\Omega = 600$, $\eta_1 = 0.95$, using the method presented in Donner & Brandenburg (1990). For the distributions of thermal and relativistic electrons we assumed a parabolic profile extending to the boundary of the halo. (Assuming a relativistic electron density corresponding to equipartition between the energy densities of cosmic rays and magnetic field did not change the results significantly.) In Fig. 5 we show for a short time interval the evolution of the poloidal and toroidal magnetic field, together with the rotation measure for the same run as in Fig. 2. The first row shows field lines of the poloidal field and the second row contours of the toroidal field strength (dotted contours denote negative values, i.e. B_ϕ points opposite to the direction of rotation). The third and fourth rows show the azimuthal dependence of the rotation measure at two different radii (projected onto the galactic plane: $r = 0.4$ and $0.6\,R$) and for an inclination angle i=30°. Note that at certain times (e.g. for $t = 5.94$) the RM curve shows a doubly peaked oscillation which would be conventionally interpreted as caused by a nonaxisymmetric field ($m = 1$). However, in our case the fields are, of course, purely axisymmetric and it is the superposition of fields from the halo and the disc that causes the simple interpretation of the RM curves in terms of axisymmetric and bisymmetric fields to become questionable in some special cases.

In Fig. 6 we compare the variation of the parity parameter with the time intervals where the azimuthal variation of the rotation measure shows a double peak behaviour. The relative duration of the double peak is approximately 30% which is quite significant. It can be expected, however, that this effect will be weaker if the poorly known electron distribution is more concentrated to the disc, in which case the effect of the halo becomes observationally less important. On the other hand, at longer wavelengths of about 20 cm the radio emission from the disc can be depolarised due to Faraday dispersion, so that the observed polarised emission of a spiral galaxy might originate at large heights above the disc (Beck, 1991b).

From Fig. 5 we see that the double peak behaviour typically occurs when P has a local maximum, i.e. when the field has maximal symmetry with respect to the equator. For the rest of the time the toroidal field is more antisymmetric close to the disc plane (e.g. for $t = 5.88 - 5.92$). We note that axisymmetric pure parity fields can show also a double peak (Donner & Brandenburg, 1990), but this effect is less dramatic than in the case of the mixed parity solutions of Fig. 5.

8. Discussion and conclusions

Our results reported above confirm, at a qualitative level, that chaotic motions and differential rotation of the gas in the halos of spiral galaxies can act as a turbulent dynamo generating a magnetic field with a scale of the order of the halo size.

The galactic halos are, therefore, the largest known objects that host a mean-field dynamo. Galaxy clusters may host even larger scale dynamos, but would, however, generate only chaotic magnetic fields; see Ruzmaikin et al. (1989). Due to the large size of the dynamo volume, the dynamo time scale is comparable to the Hubble time. As a result, the dynamos in the galactic halos are expected to be unique among astrophysical dynamos in that they are probably in a transitional regime, and the ultimate steady state has not been attained during the galactic lifetime. This may allow a memory of the initial seed field to influence the observed fields. (On purely topological grounds, if the seed field were of large scale, we might anticipate it being a mixture of A0 and S1 fields.)

Therefore, the problem of the structure and evolution of the regular magnetic field in the galactic halos requires more than analysis of the dynamo eigensolutions and/or the stability analysis of the steady solutions. For instance, our results here show that, during a prolonged period comparable to the galactic lifetime, the magnetic fields near (and within) the disc and in the halo have different symmetries with respect to the galactic equator, even and odd, respectively. Of course, a steady state reached in the limit $t \to \infty$ usually has a pure parity throughout the whole volume of the disc+halo system. (Note, however, that for a narrow range of relevant parameters mixed-parity steady-state solutions are also possible.) For the disc and halo parameters chosen here, this eventual parity is odd but it could be even if the dynamo in the disc were strong enough.

The preference for an even parity magnetic field within the disc and an odd parity field in the halo should result in asymmetry of the z-distribution of the overall magnetic field strength at times comparable with a galactic lifetime; the asymmetry is expected to be the strongest between the two transitional layers just above the disc surface (see also Moss & Tuominen, 1990; Sokoloff & Shukurov, 1990). The asymmetry of the expected kind is observed in both NGC 891 and NGC 4631 (see Figs 3 and 5 in Hummel et al., 1991): the polarisation intensities on both sides of the disc differ most strongly at the distances of 0.5 – 1 kpc in NGC 891 and 2 - 4 kpc in NGC 4631. The degree of polarisation also shows a pronounced asymmetry with respect to the major axis in these two galaxies. We should note that a north-south asymmetry observed in the distribution of Faraday rotation measures of extragalactic radio sources (Ruzmaikin et al., 1978) may be due to an asymmetric distribution of the regular magnetic field outside the disc in the Milky Way.

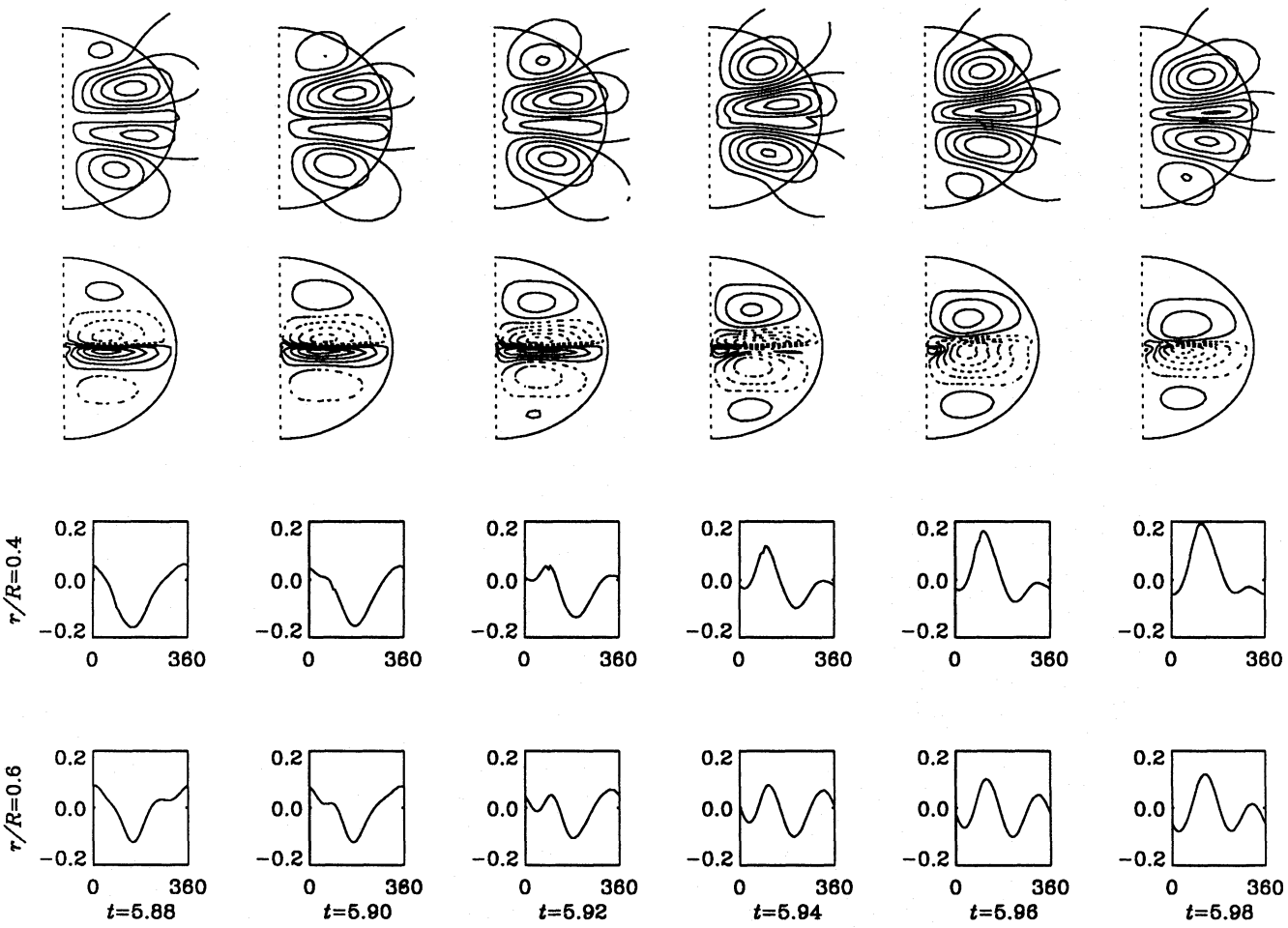

Fig. 5. Evolution of poloidal and toroidal magnetic field (upper two rows) together with the rotation measure for an inclination angle $i = 30°$ and relative radii 0.4 and 0.6 (lower two rows) for the mixed parity solution with $C_\alpha = 9$, $C_\Omega = 600$, $\eta_1 = 0.95$, $\alpha_1 = 0$, $\tilde{\alpha} = \cos\theta$

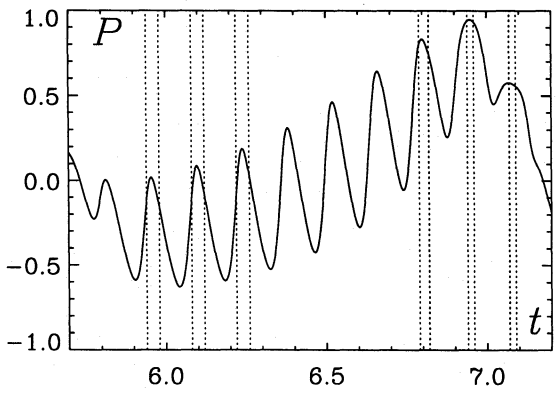

Fig. 6. Variation of the parity parameter P over one long-term cycle for $C_\alpha = 9$, $C_\Omega = 600$, $\eta_1 = 0.95$, $\alpha_1 = 0$, $\tilde{\alpha} = \cos\theta$. The vertical dotted lines denote six selected time intervals where the azimuthal variation of the rotation measure shows a double peak behaviour

Concerning particular applications of our results, it is interesting to notice that the magnetic field in the halo is oscillatory, with the period of oscillations comparable to the galactic lifetime. This oscillatory field can be described, similarly to the solar magnetic field, as a dynamo wave. The crest of the wave will in general be at different latitudes in different galaxies. This implies that one can expect to encounter a rich variety of magnetic field morphologies in the halos of spiral galaxies, e.g., with the dominance of either poloidal or toroidal field at moderate latitudes, or the field strength being maximal either at high or low latitudes, etc. It is instructive to recall in this connection that the regular magnetic fields observed in the halos of edge-on spiral galaxies NGC 891 and NGC 4631 probably have quite different structures (Hummel et al., 1991).

The mixed parity solutions presented here are similar to those found in the strictly spherical case (cf. Brandenburg et al., 1989). In both cases only the A0 solution is stable near the first bifurcation. How relevant the mixed mode solutions are is difficult to decide. If galactic dynamos operate in a very supercritical range of C_α then only S0 solutions are stable in our models. If galaxies are only slightly supercritical, then mixed modes may be possible. For example, in the range $C_\alpha < 15$, the strip where mixed modes exist has a width of about 10 percent in C_α.

Changing the value of η_1 appears to have a similar effect to changing the value of C_α in earlier investigations. Steady S0 solutions are generally more preferred when the α effect is more concentrated to the disc ($\alpha_1 < 0$). A high conductivity disc

($\eta_1 > 0$) can simulate the same effect during the start-up phase of the dynamo, when the field in the halo is still too weak. Eventually, however, the halo field becomes important and can, for suitable parameters, cause the global field to be of odd parity.

Some of our models have the interesting property that the azimuthal variation of the rotation measure can show a double peak over a significant time interval. This may be important for understanding the presence of the nonaxisymmetric fields inferred in some galaxies, because it has so far not been possible to explain such nonaxisymmetric fields as being stable solutions of the dynamo equations with axisymmetric α effect. However, this requires a rather broad distribution of thermal electrons high into the halo. Such a broad distribution is natural in a model where the dynamo activity extends throughout the halo. Finally, following our above remarks, we note that nonaxisymmetric fields might also be part of a transient solution.

Future investigations might include a more detailed study of the transient evolution for models with more realistic spatial distributions of α, α_B, η, as well as Ω. Also evolution from nonaxisymmetric initial conditions and the implications for the interpretation of the rotation measure need to be considered. Finally we mention the importance of including the effects of a galactic wind. The dynamo in the halo can be operative only provided the galactic wind is not strong enough as to advect magnetic fields away before they are amplified by the dynamo. Preliminary calculations suggest that wind speeds less than 50 km/s almost certainly will not affect our model.

Acknowledgements. The authors are grateful to Prof. Karl-Heinz Rädler for fruitful discussions at early stages of this work.

References

Beck, R.: 1990, *Geophys. Astrophys. Fluid Dyn.* **50**, 3
Beck, R.: 1991a, In *The interstellar disk-halo connection in galaxies* (ed. H. Bloemen), Kluwer Acad. Publ. Dordrecht pp.267
Beck, R.: 1991b, *Astron. Astrophys.* **251**, 15
Brandenburg, A., Krause, F., Meinel, R., Moss, D., Tuominen, I.: 1989, *Astron. Astrophys.* **213**, 411
Donner, K. J., Brandenburg, A.: 1990, *Astron. Astrophys.* **240**, 289
Elstner, D., Meinel, R., Rüdiger, G.: 1990, *Geophys. Astrophys. Fluid Dyn.* **50**, 85
Hummel, E., Lesch, H., Wielebinski, R., Schlickeiser, R.: 1988, *Astron. Astrophys.* **197**, L29
Hummel, E., Beck, R., Dahlem, M.: 1991, *Astron. Astrophys.* **248**, 23
Jennings, R. L.: 1991, *Geophys. Astrophys. Fluid Dyn.* **57**, 147
Jennings, R., Brandenburg, A., Moss, D., Tuominen, I.: 1990, *Astron. Astrophys.* **230**, 463
Krause, F., Meinel, R.: 1988, *Geophys. Astrophys. Fluid Dyn.* **43**, 95
Moss, D., Tuominen, I.: 1990, *Geophys. Astrophys. Fluid Dyn.* **50**, 113
Parker, E. N.: 1971, *Astrophys. J.* **163**, 255
Roberts, P. H.: 1972, *Phil. Trans. Roy. Soc.* **A274**, 663
Ruzmaikin, A. A., Sokoloff, D. D., Kovalenko, A. V.: 1978, *Sov. Astron.* **22**, 395
Ruzmaikin, A. A., Shukurov, A. M., Sokoloff, D. D.: 1988, *Magnetic Fields of Galaxies*, Kluwer, Dordrecht
Ruzmaikin, A. A., Sokoloff, D. D., Shukurov, A. M.: 1989, *Monthly Notices Roy. Astron. Soc.* **241**, 1
Sokoloff, D. D., Shukurov, A. M.: 1990, *Nature* **347**, 51
Sofue, Y., Fujimoto, M., Wielebinski, R.: 1986, *Ann. Rev. Astron. Astrophys.* **24**, 469
Stix, M.: 1975, *Astron. Astrophys.* **42**, 85
Sukumar, S., Allen, R. J.: 1991, *Astrophys. J.* **382**, 100
Vainshtein, S. I., Ruzmaikin, A. A.: 1971, *Astron. Zh.* (USSR), 48, 902

This article was processed by the author using Springer-Verlag LaTeX A&A style file 1990.